# Controlled Static Environment Tests on Vacuum-Membrane Solar-Dish Facets for a Low-Cost Vacuum Control System

**Duncan S. McGee[1] and Willem G. le Roux[1]**

[1] Department of Mechanical and Aeronautical Engineering, University of Pretoria, Pretoria (South Africa)

### Abstract

Small-scale vacuum-membrane facets for multi-faceted concentrated solar power (CSP) systems are investigated in this work. These facets are constructed from polymer-based reflective membranes adhered to the rim of cost-effective elliptical television antennas. Focal lengths on each facet can be varied by adjusting membrane depth. Previous studies have indicated that the membrane depth changes due to varying ambient conditions which affects the optical performance of the concentrator. The current work first focused on identifying the main cause of membrane movement using a controlled-environment experimental setup. Secondly, the work focused on how membrane movement could be reduced by utilizing a low-cost focus control system in outdoor experiments. The controlled-environment experimental setup underscored the significant influence of ambient temperature alterations on membrane movement compared to ambient pressure alterations. The outdoor experiment demonstrated substantial membrane movement; however, results showed that a low-cost constant differential pressure focus control system consisting of two 12 V diaphragm air pumps, two BMP280 barometric pressure sensors, and a microcontroller could reduce this movement to being within the targeted minimum limit of ±2 mm. It was found that periodic adjustments may be required to maintain long-term stability.

*Keywords: Vacuum-membrane, CSP, Concentrator, Low-Cost, Focus Control System*

## 1. Introduction

The University of Pretoria is actively working on the development of a small-scale concentrated solar power (CSP) system for the generation of electrical power and/or process heat (Roosendaal, et al., 2020; Swanepoel, et al., 2021). Such a system incorporates a multi-faceted solar dish concentrator that employs vacuum-membrane technology, as shown for example in Fig. 1(a). The facets constituting this innovative design are constructed from readily available and cost-effective elliptical television antennas. Over the rim of each facet, a reflective polymer-based membrane is stretched and affixed with adhesive (Roosendaal, et al., 2020). A crucial step involves creating a vacuum within each facet, a process that results in the formation of a near-parabolic shape of the membrane. What makes this system particularly versatile is its ability to accommodate variable focal lengths on each facet within the solar-dish array. This variability arises because the focal length is intrinsically linked to the membrane depth. For instance, investigations conducted by Swanepoel et al. (2020) demonstrated that altering the membrane depth from 25 mm to 5 mm can cause a substantial shift in focal length, ranging from about 2 m to 8 m.

From earlier outdoor experiments involving these facets, it became apparent that changes in the internal facet temperature, largely influenced by prevailing environmental conditions, had a pronounced impact on membrane depth (McGee, et al., 2021). Various interventions aimed at mitigating these depth fluctuations, such as filling the facets with helium or R-134a (refrigerant), or reducing the initial air volume, failed to yield a significant reduction in depth variation when compared to the original air-filled facets. However, promising results emerged from facets equipped with less-tightly pretensioned membranes, hinting at the potential to curtail overall membrane depth variations during typical operational days. Research conducted by Murphy (1987) has indicated that a thin membrane with a small modulus of elasticity and substantial pretension can approximate a nearly perfect parabolic shape. This holds true if vacuum-induced deformations do not push the


10.18086/swc.2023.03.08 Available at http://proceedings.ises.org

membrane beyond its yield point. In contrast, membranes lacking pretension tend to assume shapes closer to spheres rather than the preferred parabolic configuration, which is essential for efficient concentration of solar energy (Murphy & Tuan, 1987).

This ongoing work delves deeper into the vacuum-membrane facets integral to the multi-faceted solar dish concentrator. The objective is to systematically investigate the influence of static environmental conditions on membrane depth. This is achieved by manually manipulating the direct ambient temperature and pressure within a controlled-environment setup. The findings from this investigation promise to be invaluable in the development of an autonomous, cost-effective vacuum control system. Such a system will play a pivotal role in maintaining a consistent membrane depth during the operational phase of the CSP system, thereby enhancing its overall efficiency and performance.

## 2. Methodology

A controlled-environment enclosure was assembled using 30-mm-thick Medium Density Fibreboard (MDF). It included a removable 3-mm-thick acrylic hatch on the top to allow visibility, and this hatch was securely fastened before adjusting the internal pressure. To prevent movement due to pressure changes, an outer structure was added to reinforce the acrylic hatch, and sections of polystyrene were used for insulation on the inside. Beneath the enclosure, two 1/4-inch solenoid valves were in place, controlled by a microcontroller. These valves could either introduce high-pressure air into the enclosure to raise the internal pressure or enable a vacuum pump with a reservoir to extract air from the enclosure, reducing the internal pressure. Inside the enclosure, a heater with a built-in fan was installed, under the control of a Delta DTA4848 temperature controller. Additionally, a thermocouple was positioned in front of the fan to monitor temperature. At the centre of the enclosure, a vacuum-membrane solar dish facet was mounted. This facet comprised a polymer-based material with an aluminized reflective membrane adhered to the rim of a commercially available satellite television antenna. It was secured within a specially designed frame before closing the enclosure, with the membrane having an initial, evenly distributed pretension of 71 kg. Fig. 1 shows both the external (b) and internal (c) components of the experimental setup within the wind tunnel laboratory at the University of Pretoria, South Africa.

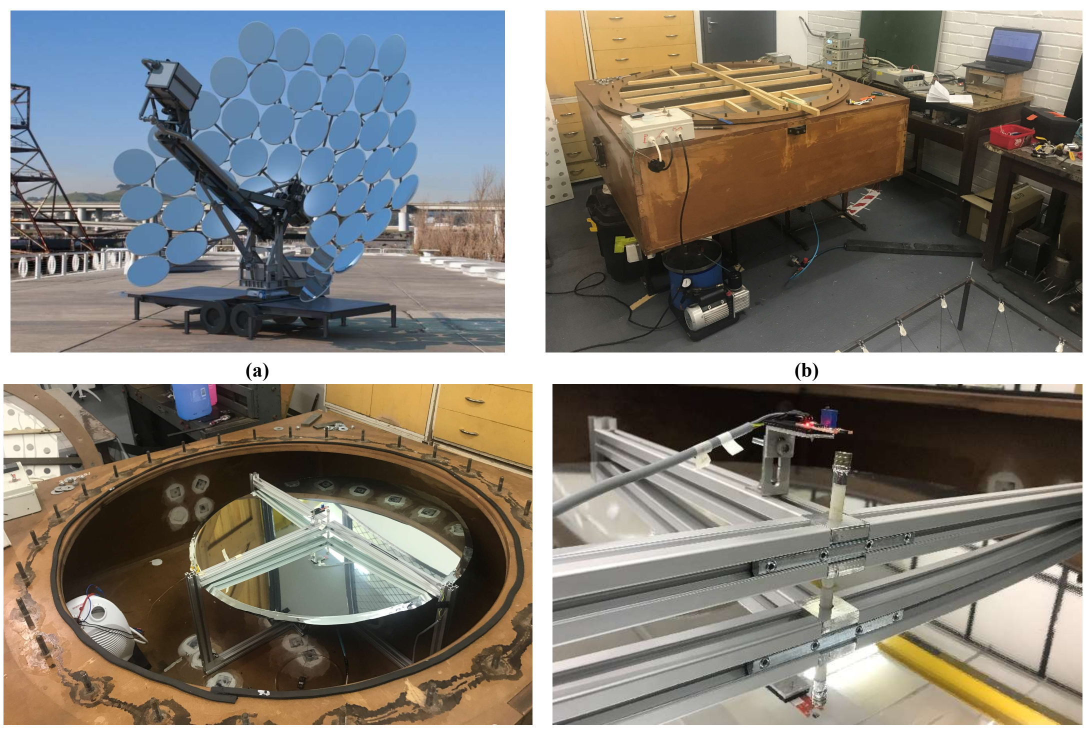

(a) (b) (c) (d)

**Fig. 1: (a) Vistualization of a CSP system under development, (b) the controlled-environment experimental setup, (c) the inside view of the setup, and (d) the Hall effect module mounted on the support frame at the exact centre of the reflective membrane.**

The facet support frame was specifically designed to hold the dish on the factory bracket at the rear of the dish, ensuring that the facet did not make contact with any other part of the support frame. This setup replicated the mounting conditions during the actual operation of the concentrated solar power (CSP) system. The top part of the frame, which extended over the reflective membrane, was precisely aligned with the centre of the facet. At this intersection point, there was an aluminium guide that directed a plastic rod either upward or downward as the membrane expanded or contracted due to changes in the volume of the vacuumed cavity. Located at the opposite end of the plastic rod were three permanent magnets, directly positioned beneath a Hall effect module mounted on the top section of the support frame, as illustrated in Fig. 1(d). The Hall effect module measured the analog signal in volts of the magnetic strength. When the magnets were near the Hall effect sensor, the maximum voltage reading obtained was 4.3 V. As the magnets moved farther away from the sensor due to membrane contraction, the voltage reading decreased. To ensure accuracy, the Hall effect module underwent calibration using a milling machine and Digital Readout (DRO) at 0.5 mm increments, ranging from 0 mm to 25 mm. This calibration resulted in a function that correlated voltage readings to membrane depth in millimetres. To assess measurement repeatability, random voltage readings were recorded at different depths and compared with the original voltage readings, confirming an acceptable repeatability within ±0.0001 V.

In addition to monitoring the facet itself, ambient conditions outside the controlled enclosure were closely observed to understand how the direct ambient conditions of the facet inside the enclosure were altered. This involved measuring ambient temperature using a Type-T thermocouple connected to a data acquisition device (DAQ), as well as monitoring ambient pressure with a BMP280 barometric pressure module linked to an Arduino Uno microcontroller. The differential pressure between the ambient environment and the interior of the enclosure was gauged using an Omega PX277 differential pressure transducer connected to the DAQ. To determine the facet's actual ambient conditions, the differential pressure transducer reading was either added to or subtracted from the barometric sensor reading, depending on whether the enclosure was pressurized or depressurized.

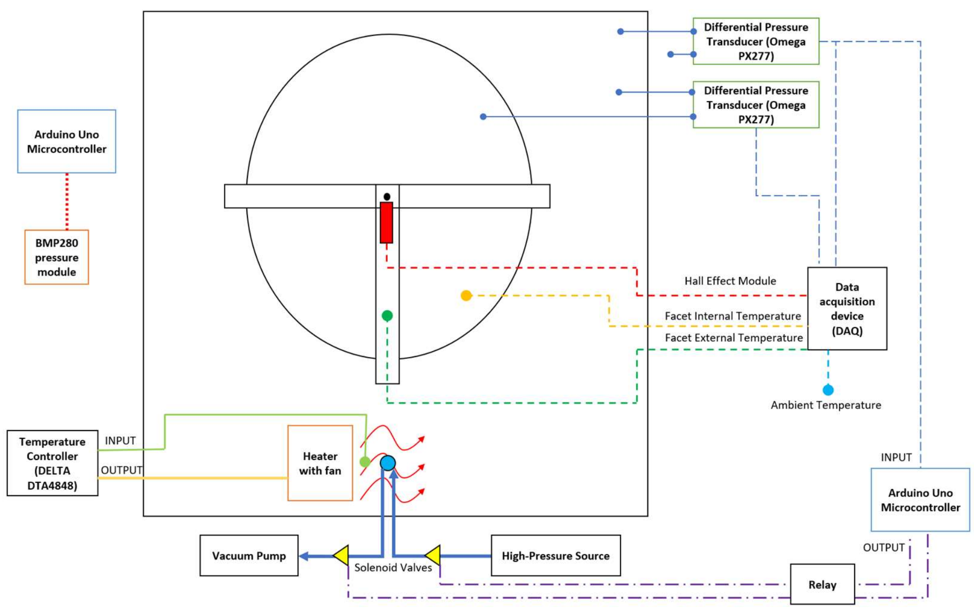


**Fig. 2: Schematic of the controlled-environment enclosure experimental setup.**

As shown in the schematic shown in Fig. 2, various measurements were taken inside the enclosure and inside the facet. A Type-T thermocouple was positioned on top of the facet support frame as close to the centre of the enclosure as possible. Additionally, the temperature within the facet itself was measured using another Type-T thermocouple, which featured a removable coupling located at the bottom of the facet. To determine the internal pressure of the facet, the differential pressure between its interior and the enclosure was measured with an Omega PX277 differential pressure transducer. All the instrumentation used to measure the facet and enclosure conditions was connected to the DAQ.

### 2.1 Ambient pressure alteration experiment

Three specific tests were conducted on the facet while it was inside the enclosure, with an initial membrane depth of approximately 10 mm. These tests involved altering the direct ambient pressure on the facet, either decreasing or increasing it and adjusting the direct ambient temperature. For the pressure experiments, the enclosure's hatch was securely bolted shut to ensure an airtight seal. The test commenced with a 20-second period of inactivity until the microcontroller activated a relay module, which in turn opened a solenoid valve connecting the enclosure to either the vacuum pump's reservoir or a high-pressure source. This action resulted in either decreasing or increasing the gauge pressure within the enclosure. The pressure was adjusted until the differential pressure transducer between the enclosure's internal and external environments registered approximately -500 Pa (gauge) or 500 Pa (gauge). At this point, the microcontroller maintained a constant pressure for 20 seconds by manipulating the solenoid valves associated with the vacuum pump or high-pressure source, depending on the necessary adjustment to stabilize the enclosure's pressure. After this 20-second interval, the microcontroller opened only the relevant solenoid valve to either pressurize or depressurize the enclosure back to its initial internal pressure.

### 2.2 Ambient temperature alteration experiment

For the temperature alteration experiment, the enclosure's hatch was placed on top without being bolted shut to ensure ventilation. This approach was adopted because initial tests had shown that sealing the enclosure tightly led to a drastic increase in internal pressure as the temperature rose, causing leaks and making it impossible to maintain the intended constant pressure. Nevertheless, the ventilation approach still yielded valuable results. The test began with a 5-minute period of inactivity, after which the temperature controller was activated. It initiated the operation of the heater and fan inside the enclosure. The heater (excluding the fan) was cycled on and off repeatedly for 25 minutes until the facet's direct ambient temperature reached approximately 318 K. This control strategy was implemented to prevent excessive heating, particularly on one side of the enclosure where the temperature controller's thermocouple was positioned directly in front of the fan. After the 25-minute period, the heater and fan were switched off, and the test continued to monitor conditions until the temperature returned to a constant room temperature.

### 2.3 Outdoor experiment

Upon studying the effects of altering static ambient conditions on membrane movement, it was suggested that maintaining a constant differential pressure might eliminate membrane movement throughout an operational day as tested by Schertz, et al. (1991). An outdoor experiment was first conducted without any focus control system to determine how the membrane would move throughout an operating day. Consequently, an outdoor experiment featuring a low-cost focus control system was also conducted on the roof of the Engineering 2 Building at the University of Pretoria, South Africa. Notably, the facet remained stationary on the roof and did not maintain a consistent angle relative to the sun, as would be the case in a CSP system (see Fig. 3).

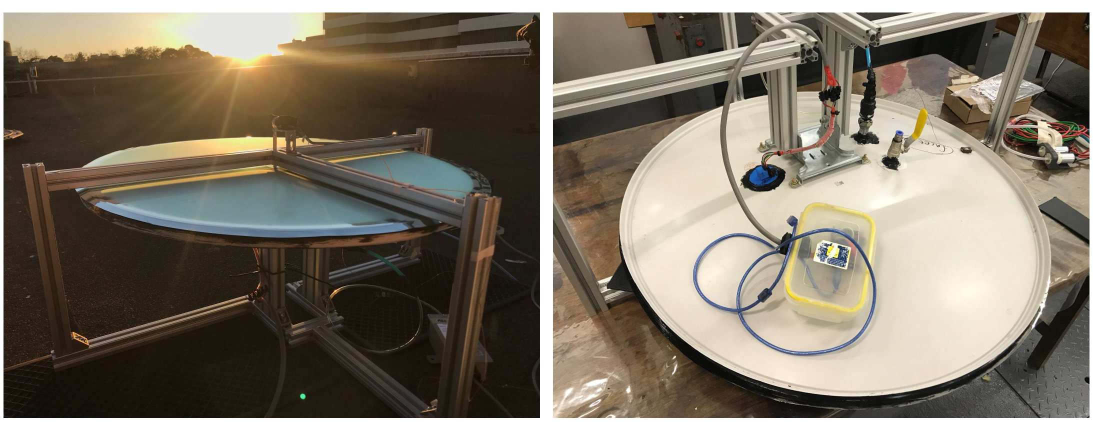

**(a)** **(b)**

**Fig. 3: (a) Outdoor experimental setup and (b) the bottom of the facet with the focus control system components.**

To maintain the differential pressure, a low-cost focus control system was employed. This controller utilized cost-effective components, including an Arduino Uno microcontroller, two BMP280 barometric pressure modules for input, and a relay module to manage two 12 V diaphragm air pumps, with one serving as a vacuum pump. Fig. 4 provides a schematic of the focus control system used to maintain the differential pressure while simultaneously monitoring internal and ambient conditions with the DAQ setup mentioned previously. The total cost of this focus control system at the time of the study was 29.34 USD. In a multi-faceted system, where one microcontroller could control multiple facets, costs could be further reduced.

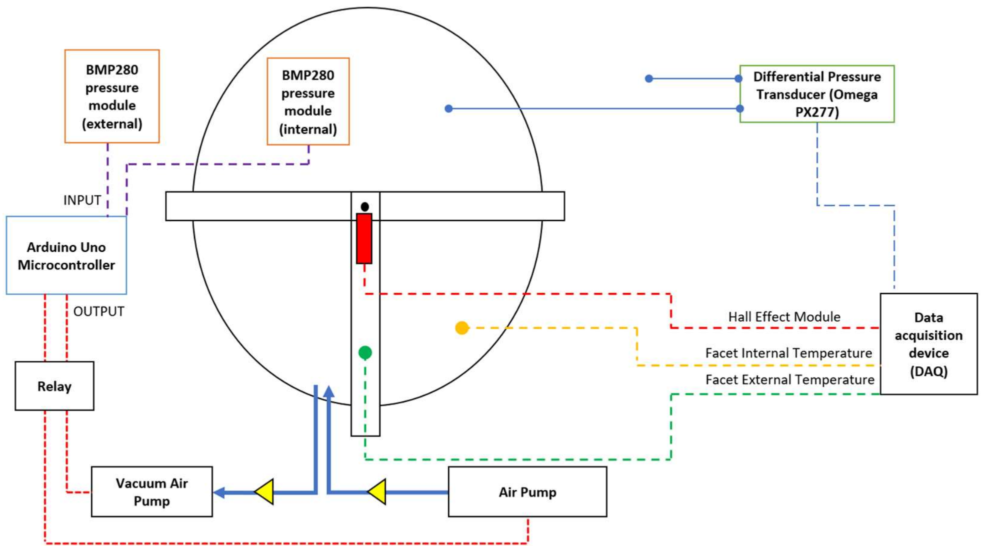


**Fig. 4: The schematic of the outdoor experimental setup.**

# 3. Results and discussion

## 3.1 Ambient pressure alteration experiment

Fig. 5 illustrates the complete test process in which the facet's direct ambient pressure decreased by about 500 Pa. The test exhibited a consistent linear decrease in the direct ambient pressure of the facet, indicating that neither the enclosure nor the top hatch deformed as the pressure changed. The membrane depth also followed a linear pattern, decreasing by approximately 0.8 mm until the facet's direct ambient pressure reached approximately -500 Pa (gauge). This pressure was then maintained as closely as possible for 20 seconds before being returned to its initial level. These isolated linear relationships are further presented in Fig. 6. During the test, it was observed that the facet's direct ambient temperature slightly decreased as the pressure decreased. This observation aligns with the principles of the ideal gas law theory. Additionally, the internal pressure of the facet experienced a slight increase during the period when the direct ambient pressure decreased. This phenomenon can be attributed to the reduction in air particles within the enclosure, exerting less force on the exterior surface of the membrane. Consequently, the remaining air particles inside the facet pushed the membrane slightly upward due to the diminished external force. This effect can be analogously compared to an inflated helium balloon ascending higher in the atmosphere, causing the balloon to expand as atmospheric pressure decreases.

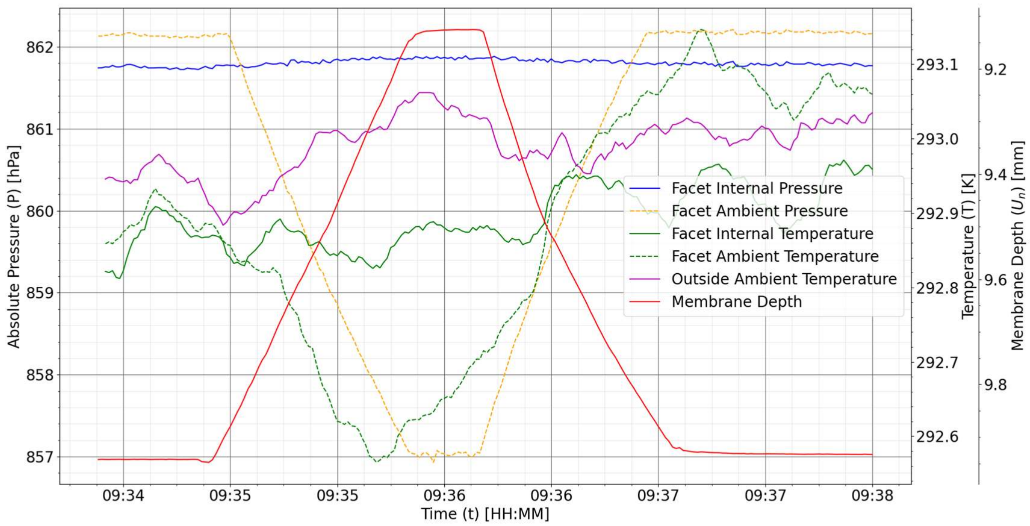


**Fig. 5: Decrease in ambient pressure test (4th of June, 2023).**

For the isolated pressure decrease and increase periods of the test, it was observed that the membrane depth deviated slightly from its initial position. This variation occurred because the change in direct facet ambient pressure had an impact on both the internal and direct ambient temperature of the facet, thereby influencing the final membrane depth. Nevertheless, this difference was minimal, and a clear linear relationship remained evident. A linear correlation of 0.14 mm/hPa was established between the membrane depth and the ambient pressure of the facet, as illustrated in Fig. 6. This implies that, with minimal temperature changes factored in, the membrane depth will decrease by approximately 0.14 mm for every 1 hPa decrease in ambient pressure.

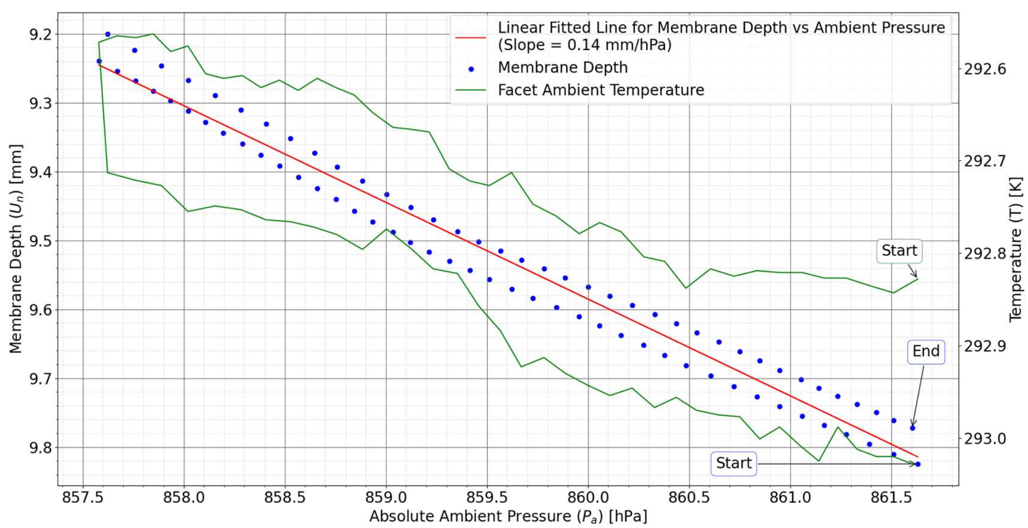


**Fig. 6: Membrane depth and internal temperature versus the decreased ambient pressure (4th of June, 2023).**

Fig. 7 presents the entire test process in which the facet's direct ambient pressure increased by 500 Pa. The test initially displayed a linear rise in the facet's direct ambient pressure, which later shifted to an exponential increase. This change suggested a slight deformation of the top hatch, although it was not a significant issue as the membrane depth also began to change exponentially during this phase. The membrane depth shifted by a total of approximately 0.7 mm downward until the facet's direct ambient pressure reached approximately 500 Pa (gauge). The pressure was then maintained as consistently as possible for 20 seconds, during which the membrane depth remained constant. Subsequently, the pressure was decreased back to its initial level, exhibiting a linear decrease in pressure and membrane depth. These isolated linear relationships are further presented in Fig. 8. It's noteworthy that the internal pressure of the facet experienced a slight decrease during the period when the direct ambient pressure was increased. This reduction in internal pressure can be attributed to the increase in air particles within the enclosure, which exerted a greater force on the exterior surface of the membrane.

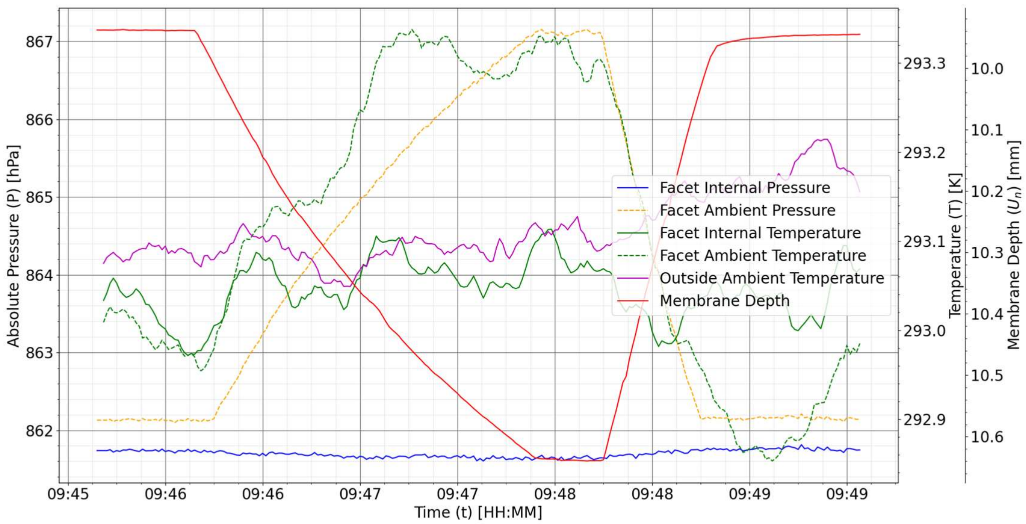


**Fig. 7: Increase in ambient pressure test (4th of June, 2023).**

For the isolated pressure increase and decrease periods of the test, it was also noted that the membrane depth was slightly off from where it started since the change in direct facet ambient pressure altered the internal and direct ambient temperature of the facet which affected the final membrane depth. However, the difference is minimal, and a clear linear relation is still notable. A linear relation of 0.125 mm/hPa was determined between the membrane depth and ambient pressure of the facet, as shown in Fig. 8. This means that the membrane depth would increase by approximately 0.125 mm if the ambient pressure increased by 1 hPa (with minimal temperature alterations). From this, it is evident that the effect of decreasing or increasing ambient pressure is almost similar since the difference is only about 0.015 mm/hPa (0.075 mm difference over a pressure alteration of 500 Pa). This difference can be due to measuring errors, linear regression errors, or due to the slight differences in temperatures during the two tests.

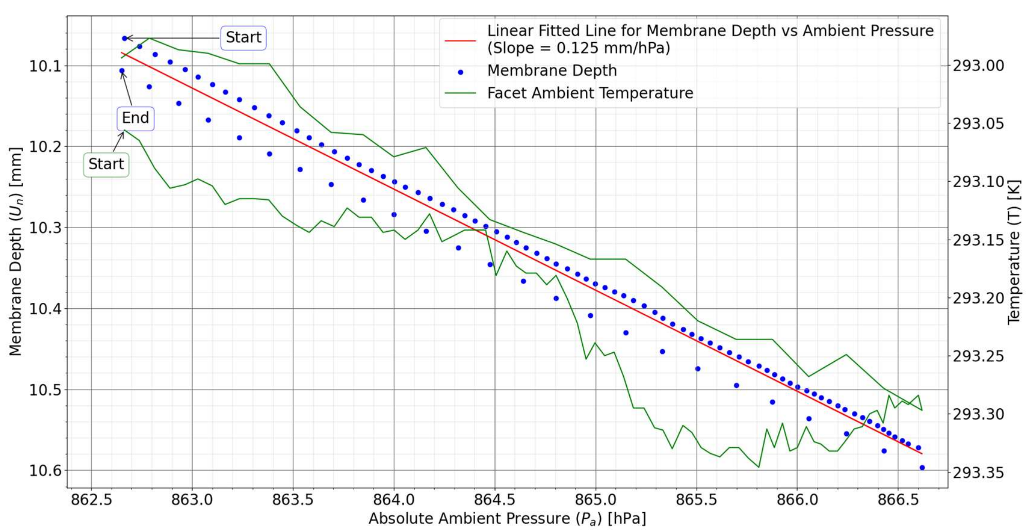


**Fig. 8: Membrane depth and internal temperature versus the increased ambient pressure (4th of June, 2023).**

## 3.2 Ambient temperature alteration experiment

Fig. 9 provides an overview of the complete temperature test conducted on the facet. The initial conditions remained constant for the first 5 minutes of the test until the heater and fan were activated. The facet's direct ambient temperature promptly rose to around 318 K, after which only the heater was periodically cycled on and off by the temperature controller, allowing the temperature to oscillate around 317 K. This resulted in the heater toggling frequently for 25 minutes, as depicted in the figure, reflecting temperature fluctuations. These fluctuations, primarily attributed to the heater, were also mirrored in the membrane's movement, indicating that temperature significantly impacts membrane motion. Upon turning on the heater, the facet's direct ambient pressure instantly increased and then gradually decreased throughout the test. During this phase, the membrane depth decreased by approximately 3.4 mm until the internal facet temperature reached 310 K. Both the internal facet temperature and membrane depth exhibited exponential growth with slight fluctuations attributed to the heater. Subsequently, the heater and fan were switched off for the cooling phase of the test, leading to rapid decreases in the facet's direct ambient temperature and pressure, facilitated by the enclosure's ventilation during the test. During the initial minutes of the cooling period, the membrane depth increased rapidly as the conditions surrounding and inside the facet reverted to their initial state.

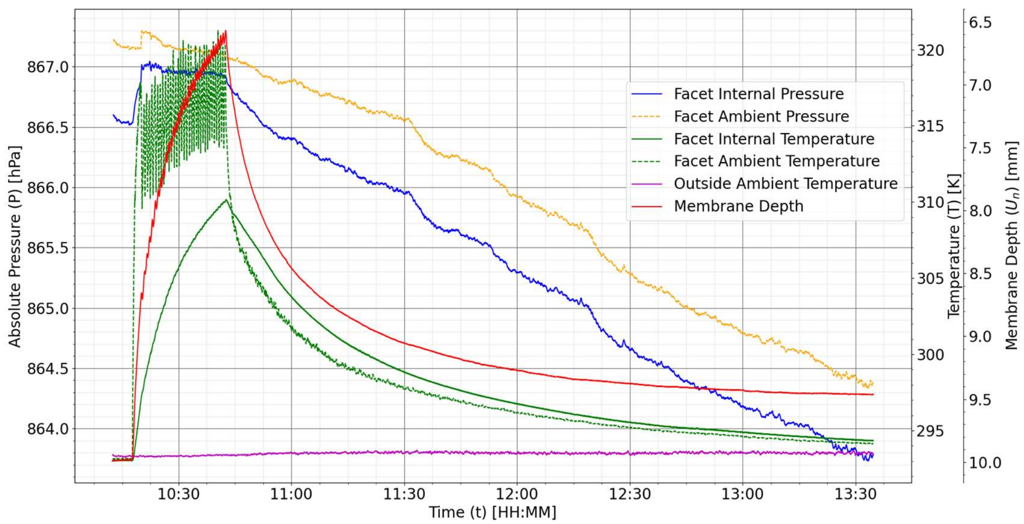


**Fig. 9: Increase and decrease in ambient temperature test (11th of June, 2023).**

During the heating period of the test, the facet's direct ambient pressure exhibited minor fluctuations within a range of 0.3 hPa, as depicted in Fig. 10. Subsequently, during the cooling period, the direct ambient pressure decreased by approximately 2.7 hPa. This indicates that ambient pressure had a minimal impact on the movement of the membrane depth during this test, contributing only -0.3375 mm to the depth, as per the findings from the earlier ambient pressure tests. The results in Fig. 10 also clearly reveal the influence of the heater cycling on and off, particularly around 317 K. Notably, there is a linear relationship between membrane depth and ambient temperature during the cooling period, spanning from 310 K to 294 K. To enhance clarity, this linear trend is isolated later in Fig. 12 for a detailed view.

Fig. 11 illustrates the behaviour of the facet's internal pressure as it increased exponentially once the internal temperature began to rise. Subsequently, as the heater's fluctuations commenced, the internal pressure exhibited a linear increase until it reached its peak at 310 K. This data showed less fluctuation compared to earlier results because the air inside the facet was not in direct contact with the heater's effects. At the start of the heating period, the membrane depth underwent an exponential decrease until it reached a depth of 8.7 mm. Following this, the depth displayed a linear fluctuation trend until reaching its minimum depth of 6.6 mm. As the ambient temperature decreased during the cooling period, the membrane depth initially increased exponentially until reaching 8.1 mm, after which it followed a linear upward trend until the end of the test. These trends suggest that the exponential patterns are indicative of transient-state heat transfer conditions between the facet and the ambient environment, while the linear trends represent steady-state heat transfer conditions. During real operation, the facet is likely to experience steady-state heat transfer since changes in ambient conditions are not as sudden as the rapid on or off switching of the heater.

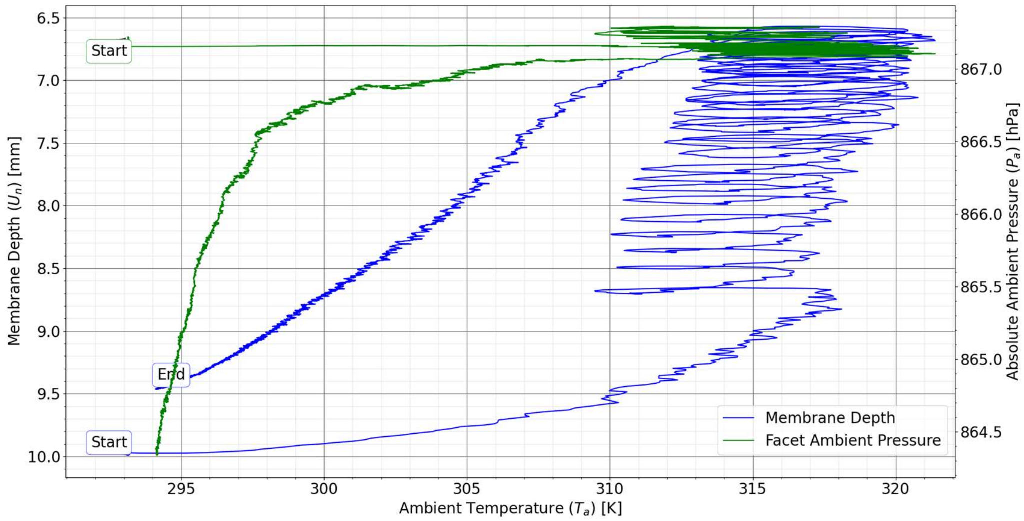


**Fig. 10: Membrane depth and ambient pressure versus the ambient temperature (11th of June, 2023).**

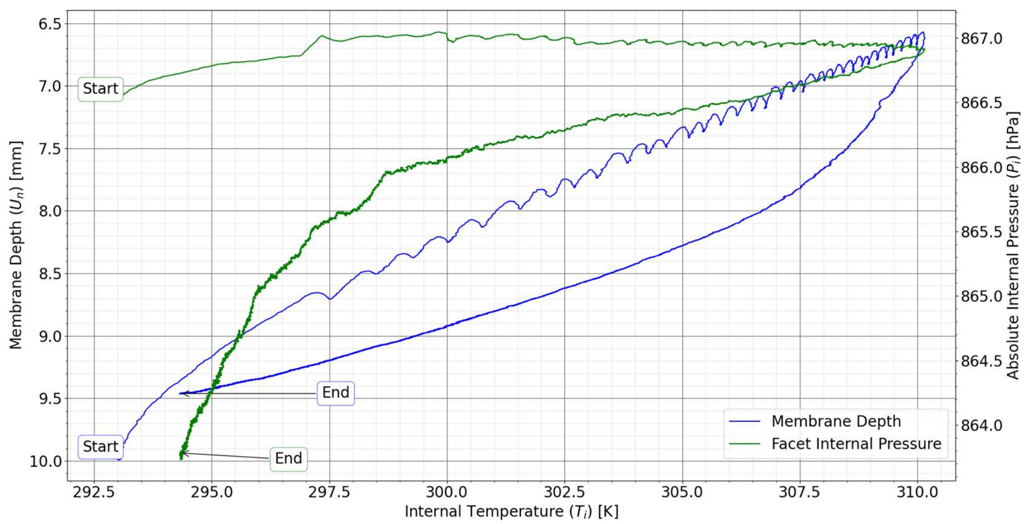


**Fig. 11: Membrane depth and internal pressure versus the internal temperature (11th of June, 2023).**

Fig. 12 presents the isolated steady-state heat transfer data observed during the temperature test of the facet. During the heating period of the test, a linear relationship was established, indicating that the membrane depth and internal temperature were related at a rate of 0.159 mm/K. Conversely, during the cooling period, another linear relationship was identified, with the membrane depth and internal temperature having a rate of 0.102 mm/K. Additionally, during the cooling period, a linear relationship emerged between the membrane depth and ambient temperature, indicating a rate of 0.133 mm/K. This implies that the membrane depth will increase by approximately 0.133 mm for every 1 K decrease in ambient temperature, assuming minimal pressure alterations.

Based on the findings presented in this section, it is evident that ambient temperature has a more significant influence on membrane movement compared to ambient pressure during an operational day. In the context of a winter's day in Pretoria, South Africa, where ambient conditions can be expected to change by approximately 3 hPa in terms of pressure and about 15 K in terms of temperature, the effect on membrane depth can be estimated. Specifically, the membrane depth is projected to change by approximately 0.398 mm due to variations in ambient pressure and approximately 1.995 mm due to changes in ambient temperature, assuming no dynamic effects from radiation and convection are considered. These estimates underscore the substantial impact of temperature fluctuations on membrane movement in comparison to changes in ambient pressure.

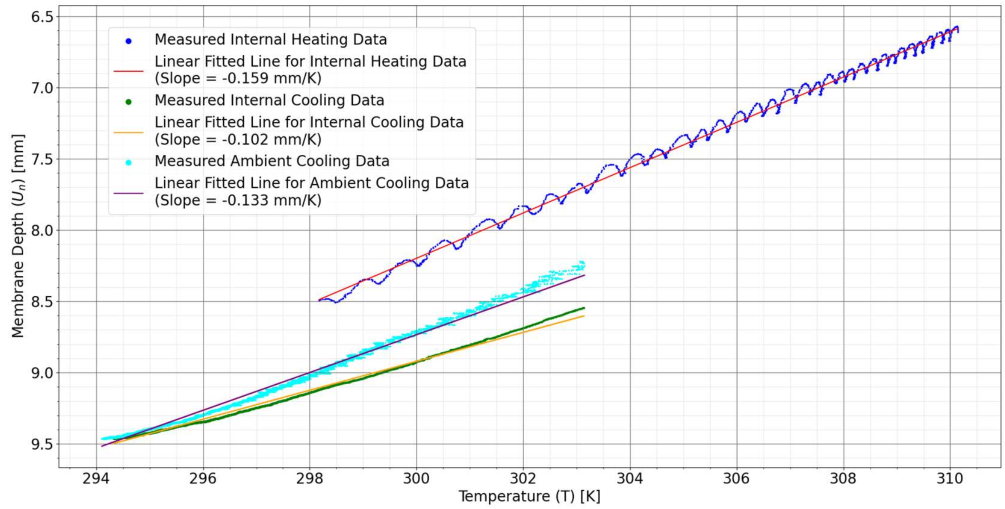


**Fig. 12: Isolated linear trends of the membrane depth versus temperature (11th of June, 2023).**

## 3.3 Outdoor experiment.

The outdoor test results, conducted without a focus control system, clearly indicate significant membrane movement, with a maximum depth reduction of 4 mm during an operational day, as demonstrated in Fig. 13. At the shallowest depth of 6 mm, the ambient pressure decreased by about 1.3 hPa and the ambient temperature increased by about 17.5 K. From the controlled-environment enclosure test, the membrane depth decreased by about 2.5 mm due to static ambient conditions, indicating that the remaining 1.5 mm is possibly due to the dynamic ambient conditions. The internal and ambient temperatures closely mirrored each other throughout the day, suggesting the presence of steady-state heat transfer conditions, consistent with the controlled-environment experimental results. It's worth noting that the internal facet temperature had a significant impact on membrane movement, as evidenced by the close resemblance between the profiles (red and green lines), aligning with the findings from the controlled-environment tests.

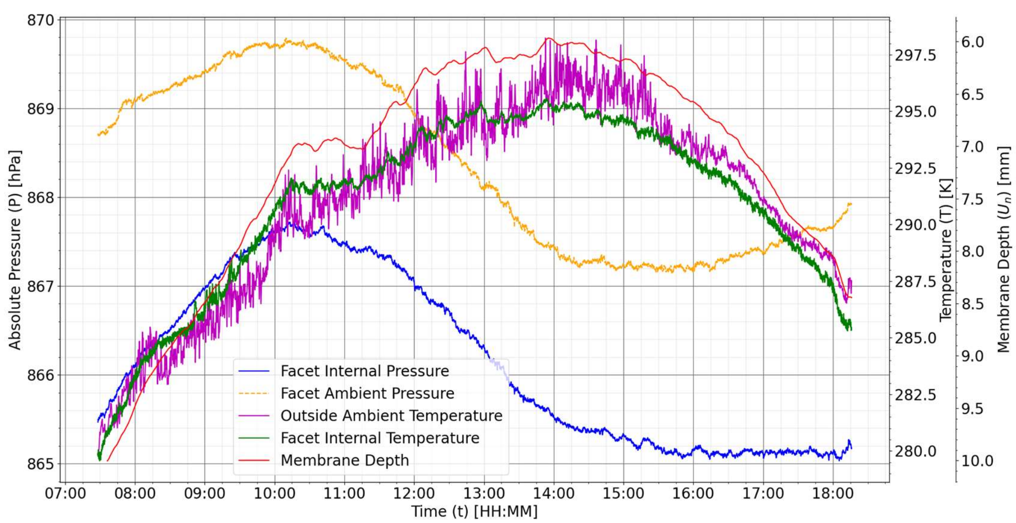


**Fig. 13: Outdoor experiment results without a focus control system (1st of July, 2023).**

A linear relationship was found between membrane depth and internal temperature, with a relation of 0.277 mm/K (see Fig. 14). This linear trend persisted even as the temperature decreased after reaching its peak at around 295 K. Comparing this result to the controlled-environment test (0.159 mm/K), it's evident that the outdoor relation is 74% higher. This difference is likely due to the influence of radiation and convection effects which are present outdoors, factors which were not considered in the controlled-environment tests. This suggests that static ambient conditions contributed to about 57% of the internal conditions, with the remaining 43% influenced by dynamic effects like radiation and convection.

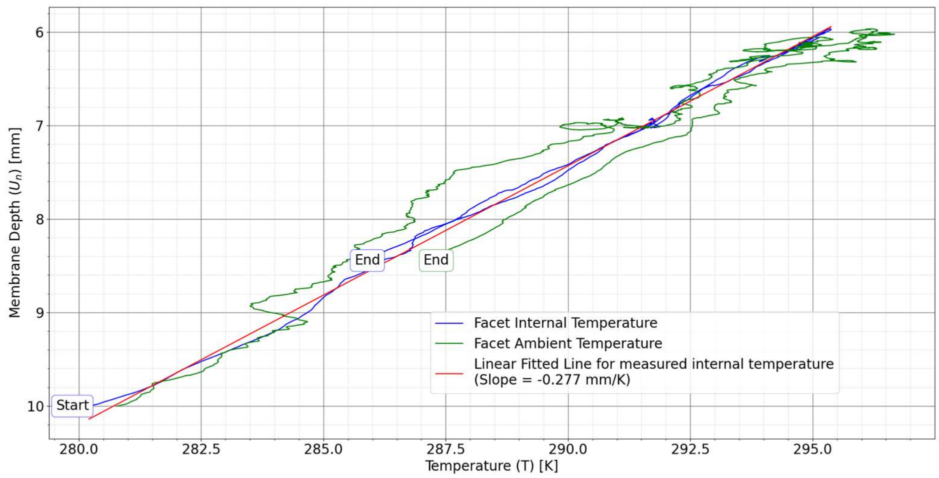


**Fig. 14: Membrane depth versus temperature during the outdoor experiment without a focus control system (1st of July, 2023).**

In the outdoor test of the controlled facet, which maintained a constant differential pressure utilizing the low-cost focus control system, the membrane movement exhibited a notable reduction compared to the uncontrolled facet throughout an operating day, as illustrated in Fig. 15. The test began with a membrane depth of approximately 11.1 mm at 06:40 and reached a peak value of 12.7 mm around 09:00. Subsequently, the membrane depth gradually decreased to a minimum of 9.6 mm at 18:00. This indicates that the membrane depth experienced increases and decreases of about 1.6 mm and 1.5 mm, respectively. These variations fall within the 2 mm accuracy threshold required for achieving a targeted minimum intercept factor of 90%, as determined by Roosendaal et al. (2021). It's worth noting that Roosendaal et al. emphasized the sensitivity of the intercept factor to negative adjustments, making the observed 1.5 mm change just within the specified limit.

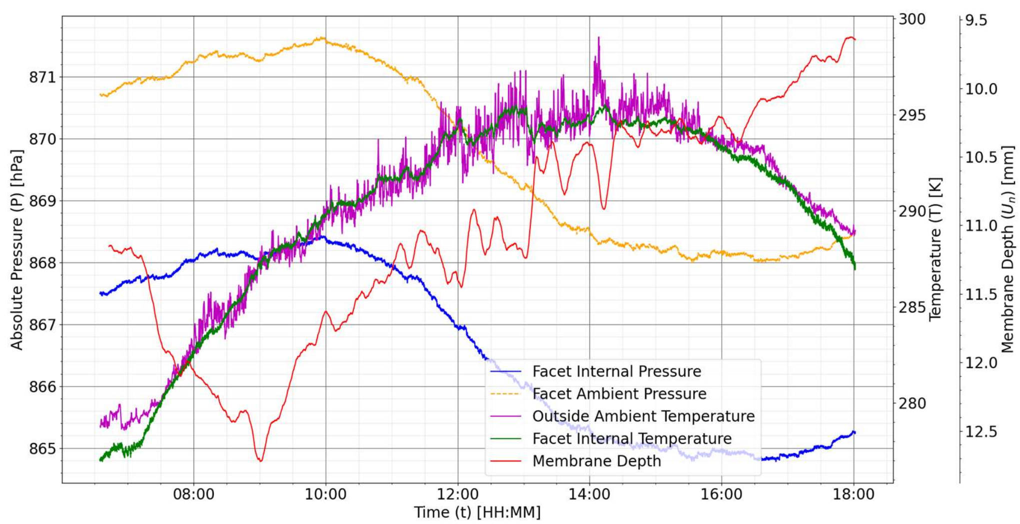


**Fig. 15: Outdoor experiment results with constant differential pressure focus control system (3rd of July, 2023).**

Maintaining a constant differential pressure for the facet doesn't guarantee long-term operation on a CSP system without adjustments. As seasons change, ambient pressure fluctuates, necessitating periodic control system resets, potentially at the start of each season or even weekly, depending on extended tests. The membrane depth should ideally remain constant when differential pressure is constant. However, the membrane material's stiffness, affected by temperature changes, complicates this ideal scenario. Polymer-based membranes stiffen at lower temperatures and soften at higher ones. This means that relying solely on differential pressure control may not be effective for polymer-based reflective membranes, unlike metal-based membranes like the SKI facet (1991), which are less sensitive to temperature changes.

## 4. Conclusion and recommendations

In conclusion, this research reveals the relationship between ambient conditions and membrane movement in solar concentrating systems. Controlled ambient pressure experiments demonstrated linear connections between pressure changes and membrane depth, with decreasing and increasing pressure affecting the membrane similarly. However, controlled ambient temperature experiments revealed a more substantial influence on membrane behaviour. Temperature fluctuations had a pronounced impact on membrane movement, with both heating and cooling periods showing linear relationships between temperature changes and membrane depth. Comparing the effects of ambient pressure and temperature, it became clear that temperature fluctuations had a more significant impact during an operational day. Outdoor experiments without a focus control system showcased substantial membrane movement during the day, with significant temperature-dependent effects. In contrast, outdoor tests with a constant differential pressure focus control system exhibited reduced membrane movement, but maintaining constant pressure alone is insufficient for long-term stability. Periodic control system adjustments may be necessary due to seasonal changes, especially for polymer-based reflective membranes, which are sensitive to temperature variations.

Further exploration of the constant differential pressure focus control system is advisable, with a focus on integrating temperature-related effects on membrane stiffness. This can potentially lead to a more significant reduction in overall membrane movement. Additionally, it is recommended to explore an alternative focus control system that continuously monitors membrane depth. This approach would mitigate challenges arising from dynamic pressure effects caused by wind and temperature-induced material stiffness variations. Furthermore, investigating various vacuum-membrane construction methods, including considerations such as pretension, membrane thickness, and facet size, may help further minimize membrane movement.

## 5. Acknowledgements

The authors express their gratitude to the Renewable Energy Hub and Spokes Program of the Department of Science and Innovation (DSI) for financial support through the UP Solar Thermal Spoke.

## 6. References

McGee, D.S., Roosendaal, W. & Le Roux, W.G., 2021. Environmental Investigation of Vacuum-Membrane Solar-Dish Facets. (Online), 27th SolarPACES Conference. 27 September – 1 October.

Murphy, L.M., 1987. Moderate Axisymmetric Deformations of Optical Membrane Surfaces. Journal of Solar Energy Engineering, 109(2), pp. 111-120. https://doi.org/10.1115/1.3268187

Murphy, L.M. & Tuan, C., 1987. The formation of optical membrane reflector surfaces using uniform pressure loading (Report: SERI/TR-253-3025), Golden: Solar Energy Research Institute.

Roosendaal, C., Swanepoel, J.K. & Le Roux, W.G., 2020. Performance analysis of a novel solar concentrator using lunar flux mapping techniques. Solar Energy, Volume 206, pp. 200-215. https://doi.org/10.1016/j.solener.2020.05.050

Roosendaal, C., Swanepoel, J.K. & Le Roux, W.G., 2021. Optical modelling of a vacuum-membrane solar dish based on elliptical television antenna. Southern African Sustainable Energy Conference, Stellenbosch, 17–19 November.

Schertz, P.T., E., P., Brown, D.C. & Konnerth III, A., 1991. Facet Development for a Faceted Stretched-Membrane Dish by Solar Kinetics Inc. (Report: SAND91-7009), Albuquerque: Sandia National Laboratories.

Swanepoel, J.K., Le Roux, W.G., Lexmond, A.S. & Meyer, J.P., 2021. Helically coiled solar cavity receiver for micro-scale direct. Applied Thermal Engineering, Volume 185, p. 116427. https://doi.org/10.1016/j.applthermaleng.2020.116427

Swanepoel, J.K., Roosendaal, C. & Le Roux, W.G., 2020. Photogrammetry Analysis of a Vacuum-Membrane Solar Dish Using Elliptical Television Antennas, (Online) 26th SolarPACES Conference, 28 September–2 October. https://doi.org/10.1063/5.0087025